Regular Article

Kaythar A. Ibrahim*, Suhaib Y. Al-Darzi and Mohammed H. Shukur

Effect of openings on simply supported reinforced concrete skew slabs using finite element method

https://doi.org/10.1515/eng-2022-0464
received January 28, 2023; accepted May 07, 2023

Abstract: Reinforced concrete skew slabs are commonly used in bridges due to space constraints in motorways and in congested urban areas. Such slabs also often need to contain openings for architectural requirements or services, and this study seeks to determine the effect of these openings on the strength of the skew slabs. The finite element method was used to analyze 13 cases of slabs with skew angles of 45°. The first and second cases were used to validate the results with experimental work. Other cases studied the effect of the position and shape of openings on the strength of the skew slabs under both one-point and four-point loading conditions. The study also showed that the worst location for the opening was near the obtuse corners since this is where most of the load is transferred. With respect to the shape of openings, three different shapes with the same area were used: skew, circle, and square shapes. It was found that the effect of the opening shape depends on how many steel reinforcements are removed, as well as the appearance of negative cracking brought on as a result of the opening. Overall, the square shape introduces the smallest reduction in the skew slab strength compared with a slab with no opening. Accordingly, the study recommends that the strength of skew slabs can best be maintained if square openings are employed near the acute corners, alongside negative steel reinforcement to avoid cracking.

Keywords: skew slab, reinforced concrete slab, slab opening, finite element method

1 Introduction

Concrete slabs find widespread application in the construction of floors in residential and commercial settings and bridge decks. Due to the potential savings in labor and formwork expenses that can be achieved by omitting girders, reinforced concrete (RC) slab bridges are preferred for short spans [1].

A four-sided slab with equal opposite angles that are not at 90° is referred to as a skew slab. These skew slabs are commonly used in highway bridges [2] due to space restrictions, and demand for skew slabs or bridges have also risen in densely populated urban areas [3–5].

The skew angle (α) is typically calculated clockwise from the vertical line perpendicular to the skew slab's support line. The ratio of the span to the width of the supports, meanwhile, is known as the aspect ratio (r). The right span is the distance between the two parallel lines of supports, while the skew span is the span of a skewed slab measured along an unsupported edge of the design [6]. Due to the structure's skewness, the stress and deflection characteristics are very different from those seen in slabs at a right angle [7]. Indeed, the force flow in skew slabs is significantly more complicated than in straight slabs [8,9], and analysis of the RC nonlinear zone is especially challenging and, in some cases, impossible, due to the complicated behavior of RC [10]. In right-angle slabs, the load path travels directly in the direction of the support toward the span while in the skew slab, the load goes straight to the skew slab's obtuse corners [11]. The moment field induced in the slab as a result of the applied load controls the design of any RC slab. This moment field in skew slabs changes a lot depending on the skew angle, slab aspect ratio, and boundary conditions [12].

* **Corresponding author: Kaythar A. Ibrahim,** Environmental Engineering Department, College of Engineering, University of Mosul, Mosul City, Iraq, e-mail: kaythar6871@uomosul.edu.iq
Suhaib Y. Al-Darzi: Civil Engineering Department, College of Engineering, University of Mosul, Mosul City, Iraq, e-mail: suhaib.qasim@uomosul.edu.iq
Mohammed H. Shukur: Environmental Engineering Department, College of Engineering, University of Mosul, Mosul City, Iraq, e-mail: m.h.alkafaf@uomosul.edu.iq

Numerous techniques are used to analyze slabs, including grillage and finite element approaches. Grillage analysis is typically the approach utilized in bridge analysis, where an equivalent grillage of beams is substituted for the deck [13] while the finite element method depends on dividing the geometry of the structure into discrete finite elements and solving it together to find the solution.

Roll and Aneja [14] examined the performance of straight and skew bridge models and constructed using a simply supported box beam. The purpose of their testing was to investigate whether or not finite-element modeling was accurate.

A method for estimating moments in continuous normal and skew slab-and-girder bridges that are caused by live loads was provided by Khaleel and Itani [15]. Menassa et al. [5] evaluated the effect of a skew angle compared with a straight bridge. They found that bridges with skew angles of less than 20° could be designed as non-skew because the moments are practically the same for both types of bridges.

The grillage approach and the finite element method of analysis were compared and contrasted by Khatri et al. [16]. The authors concluded that the finite element method achieved a closer agreement with the exact solution.

Kar et al. conducted research showing that when the skew angle increases, the stresses in the slab change noticeably compared to those in a straight slab. Specifically, skewed slabs are prone to warping since the maximum stress planes are not parallel to the road's centerline. This means that the reactions at the slab support's acute end are greater than those at the other end. When the skew angle reaches around 60°, the reaction at the acute angle corner results in zero pressure. In contrast, the reaction at the obtuse angle corners is twice the level of the average reaction. This is important since it means that there are more opportunities for corner upliftment as the skew angle rises. Furthermore, according to Kar et al. [17], as the skew angle increases, the bending moment drops; compared to the right bridge in their study, it fell by almost 75%. On the other hand, while the transverse moment rises as the skew angle increases, once that angle reaches a certain level it begins to fall again.

In 2015, Kothari and Murnal found that the skew angles had a substantial impact on the seismic reactions of bridges since skewness means that the bridge responds in both the direction of the applied force and in the opposite direction. This behavior is mostly the result of a coupling effect, which causes rotation and an increase in the skew angle. In addition, it was determined that as the skew angle rose, the impact of torsion and other internal forces could not be ignored. Axial forces in the outer girders grew more quickly than those in the interior girders with increased skew angle. So, at higher skew angles, external girders were more vulnerable to earthquake forces than inside girders [18].

Anusreebai and Krishnachandran [19] found that when the skew angle increases, the ultimate load of a skew slab also increases but the slab's maximum deflection decreases.

An analytical model for the design of skew slabs with arbitrary skew angles and aspect ratios was created by Sharma et al. [12]. The model shows that for the building of bridges with short diagonals bigger than the span, skew slabs simply supported along two opposite parallel sides and free along the other two sides are adequate. The created model experimentally and numerically supports the assumptions made regarding the collapse loads and crack patterns. The study makes it easier for engineers to construct skew slab bridges without deviating from the road's alignment for any skew angle and aspect ratio.

Hussein et al. [20], meanwhile, tested four potential techniques to counteract the adverse effect of openings on the mechanical properties of slabs. Four of the six RC slabs in their study were strengthened using various carbon fiber-reinforced polymer (CFRP), steel plates, steel bars, and near-surface mounted Engineered Cementitious Composite (ECC) with steel mesh. The remaining two slabs were produced as controls. All the recommended strengthening methods, apart from ECC, were able to mitigate a sizable portion of the deterioration in mechanical properties.

In 2021, Oukaili and Merie examined how adding an opening near a column affected the punching shear resistance of RC bubbling slabs, and how well strengthening with CFRP sheets performed in mitigating those effects [21]. The experimental program was designed to investigate the impact of the opening's size, location, and separation from the column, and the positioning of bubbles in relation to the two-way critical shear section. The test results showed that the bubbled slabs' load-carrying capacity was lower than that of the reference solid and that the development of an opening close to the loaded area had a detrimental effect. The use of CFRP strengthening sheets improved the service and ultimate load capabilities, and they were also able to demonstrate that a model created by the finite element program, ANSYS, returned results that agreed well with their experimental test.

Al-Rousan [22] examined the flexural behavior of one-way RC slabs with various opening dimensions and the strengthening effect of CFRP ropes with various heating levels. It was discovered that the size of the produced opening and the exposure temperature influenced the extent to which CFRP ropes were able to mitigate the loss of mechanical properties arising from the presence of the opening. Furthermore, reinforcement with CFRP

ropes was found to minimize the percentage capacity reduction in the slab. Additionally, increasing the temperature values by two times what was observed for the yielding stiffness has a greater impact on initial stiffness.

Although openings are regularly required in RC slabs for architectural requirements or for services, to the best of the author's knowledge, no studies have been conducted to investigate the effect of openings in skew slabs. The main objective of this study, therefore, is to investigate the effect of openings on the mechanical properties of skewed RC slabs.

2 Description of structures

In this work, the modeling of RC skew slabs was based on experimental data obtained from the research conducted by Miah and Khasro [7]. The model has two opposites, which are simply supported, and has a 45° skew angle. The thickness of the slab was 75 mm, and the right span of the slab was 1,200 mm from one support center to the other, as shown in Figure 1. The actual diameter and yield strength of steel were 8.4 mm and 280 MPa, respectively.

The reinforcement steel arrangement of the skew slab is shown in Figure 2, and the clear bottom cover was 12 mm. Two cases of loading were considered in this experimental work [7]. The first was a single-point load (S1), and the second was a four-point load (S2), as shown in Figure 3. Steel plates with a width of 100 mm were used for the simple supports of the skew slab. The concrete strength of S1 and S2 was 26.5 and 28.5 MPa, respectively.

3 Modeling of skew slab

The finite element method was used to simulate the skew plate using ANSYS software. The Solid65 element in ANSYS was used to simulate the concrete. This element

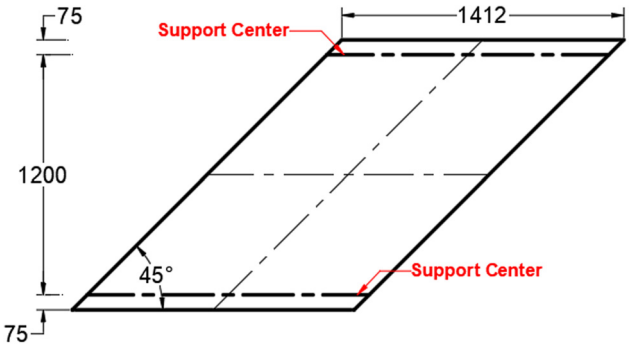

Figure 1: Skew plate geometry.

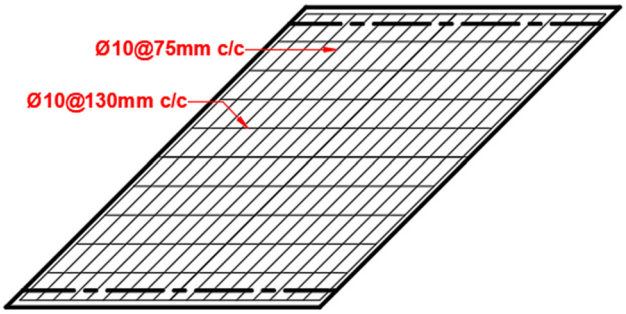

Figure 2: Skew plate steel reinforcement.

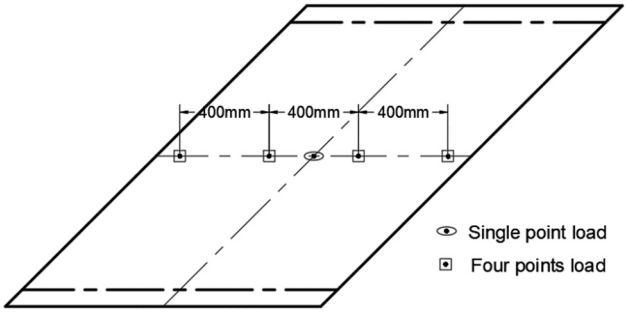

Figure 3: Loading position.

contains eight nodes, each with three degrees of freedom, referred to as the nodal x, y, and z translations. This component can undergo plastic deformation, crack in three orthogonal directions, and be crushed. The LINK180 element was used to symbolize the steel reinforcement. In the x, y, and z directions, the LINK180 element possesses three degrees of freedom: u, v, and w.

The modeling of the loading steel pad (100 mm × 100 mm) and steel support was accomplished with SOLID185. SOLID185 is a three-dimensional element for representing isotropic solids. Each node has three translational degrees of freedom in the x, y, and z nodal directions. Additionally, SOLID185 can represent prism, tetrahedral, and pyramid degeneration in irregular regions. There is a potential for distributed surface loads to act upon the element's surfaces (pressures), and the element can be used to alleviate

Table 1: Finite element input data

Value	Concrete	Steel
Modulus of elasticity	$4{,}700\sqrt{f'_c}$ [26]	200,000 MPa [27]
Poisson's ratio		0.3 [27]
Ultimate uniaxial tensile strength	$0.62\sqrt{f'_c}$ [26]	F_y = 280 MPa
Stiffness multiplier for cracked tensile condition	0.7	—

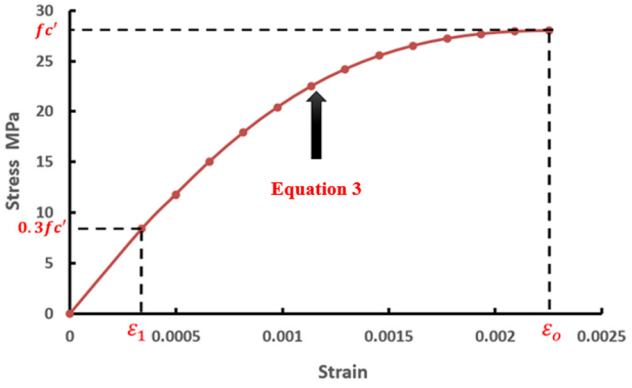

Figure 4: Uniaxial stress–strain curve for F_c' = 28.5 MPa [28].

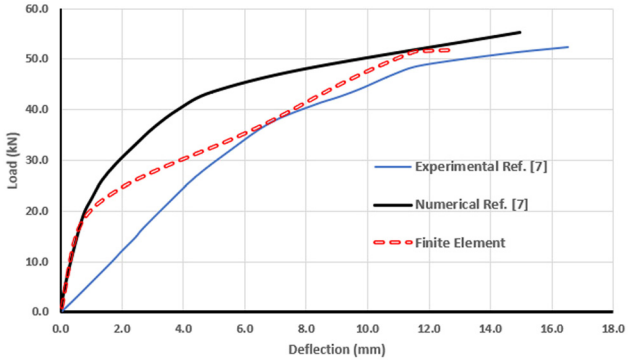

Figure 5: Verifying finite element results with other results for the case of one-point loading (S1).

problems such as large deflections, large strains, plasticity, and creep. The open and closed shear transfer coefficients in the finite element analysis should be within zero and unity [23,24]. A smooth crack is represented by a value of 0 (no shear transfer). A rough crack has a value of 1.0 (no loss of shear transfer) [25]. In this study, these coefficients were, respectively, 0.095 and 0.95 for the single-

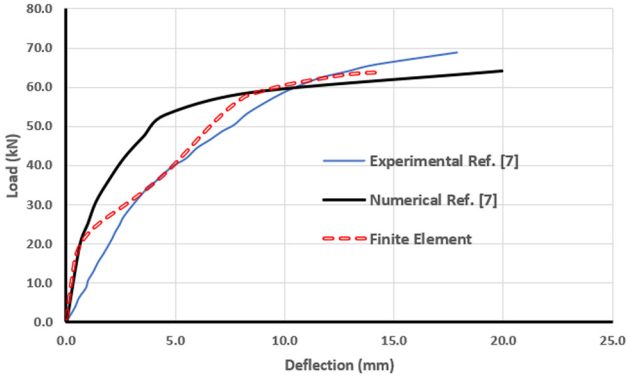

Figure 6: Verifying finite element results with other results for the case of four-point loading (S2).

Table 2: Verifying finite element results with other results for the cases (S1) and (S2)

Slab ID	S1				S2			
Measured item	Finite element	Exp. (Ref. [7])	Numerical (Ref. [7])	% Difference with experimental	Finite element	Exp. (Ref. [7])	Numerical (Ref. [7])	% Difference with experimental
First crack load (kN)	9.5	10.5	8.5	9.5	11.5	17.4	14.5	33.9
Ultimate load (kN)	51.8	52.5	50	1.3	63.9	69.0	67.0	7.4
Mid-span deflection (mm)	12.7	16.5	15	23.0	14.5	17.9	19.9	19.0

point load case (S1), and 0.3 and 0.9 for the four-point loading case (S2). Table 1 illustrates input data for the finite element.

The ANSYS software requires the concrete's uniaxial stress–strain curve. Equations (1)–(3) were thus utilized to determine the adopted (Desayi and Krishnan) stress–strain curve [26]. Figure 4 depicts the uniaxial stress–strain curve for $F_c' = 28.5$ MPa, and the curve for $F_c' = 26.5$ MPa may be found in a similar manner [26,27].

$$\varepsilon_o = \frac{2f_c'}{E_c}, \tag{1}$$

$$\varepsilon_1 = \frac{0.3f_c'}{E_c}, \tag{2}$$

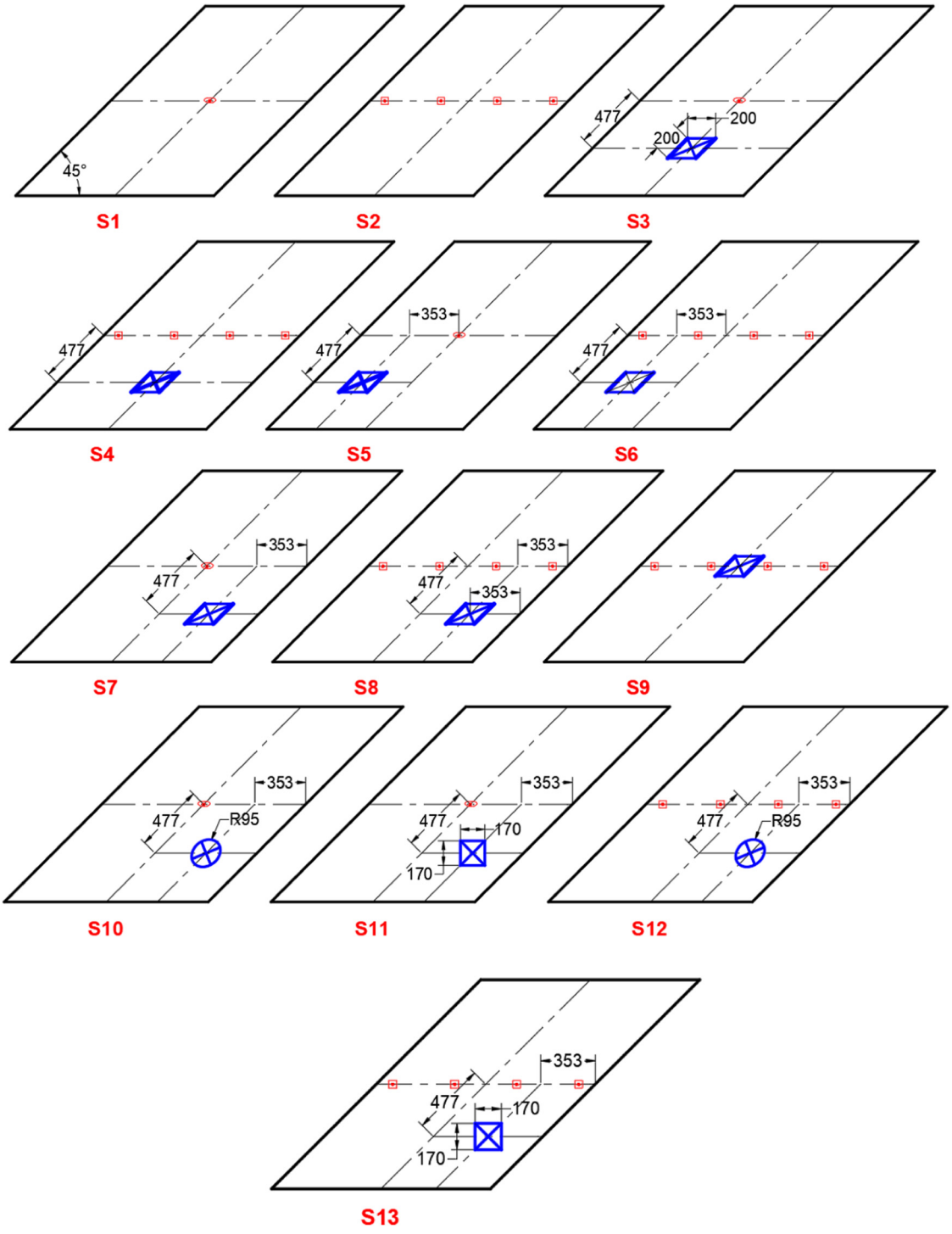

Figure 7: Studied cases of skew slabs.

Table 3: Skew slab codes and details

Slab code	Type of loading	Opening	Position
S1	One-point load	No opening	See Figure 7
S2	Four-point load	No opening	See Figure 7
S3	One-point load	200 mm × 200 mm skew opening	See Figure 7
S4	Four-point load	200 mm × 200 mm skew opening	See Figure 7
S5	One-point load	200 mm × 200 mm skew opening	See Figure 7
S6	Four-point load	200 mm × 200 mm skew opening	See Figure 7
S7	One-point load	200 mm × 200 mm skew opening	See Figure 7
S8	Four-point load	200 mm × 200 mm skew opening	See Figure 7
S9	Four-point load	200 mm × 200 mm skew opening	See Figure 7
S10	One-point load	95 mm radius circle opening	See Figure 7
S11	One-point load	170 mm × 170 mm square opening	See Figure 7
S12	Four-point load	95 mm radius circle opening	See Figure 7
S13	Four-point load	170 mm × 170 mm square opening	See Figure 7

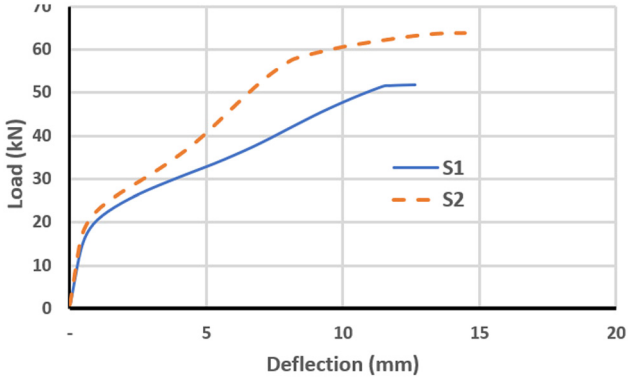

Figure 8: Load–deflection curve for S1 and S2.

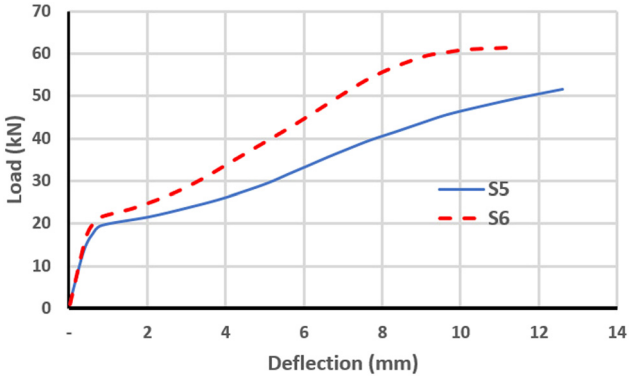

Figure 10: Load–deflection curve for S5 an S6.

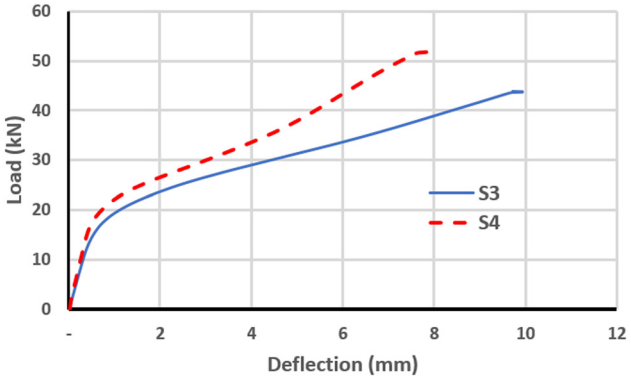

Figure 9: Load–deflection curve for S3 and S4.

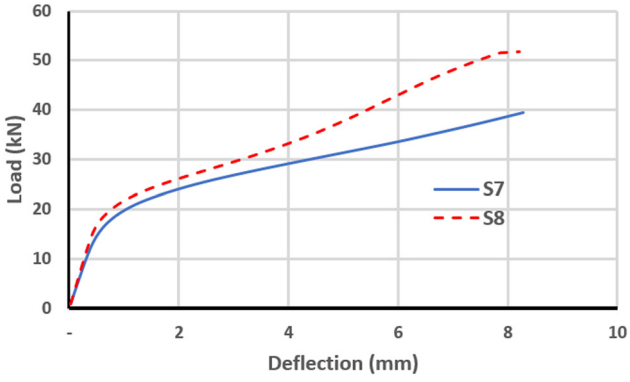

Figure 11: Load–deflection curve for S7 and S8.

$$f = \frac{E_c \varepsilon}{1 + \left(\frac{\varepsilon}{\varepsilon_0}\right)^2}. \quad (3)$$

This study used the Newton-Raphson iterative approach for the nonlinear analysis, with convergence evaluation based on the displacement norm [29].

4 Verification of finite element results

Two cases of skew slab loading, S1 and S2, were compared with the experimental and numerical works done

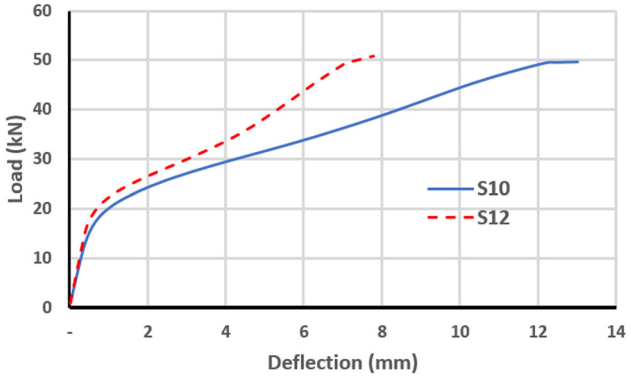

Figure 12: Load–deflection curve for S10 and S12.

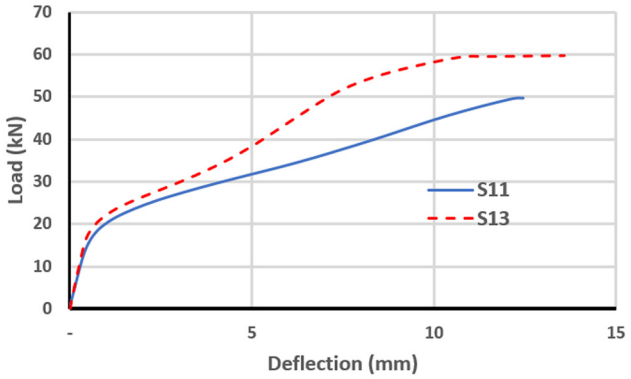

Figure 13: Load–deflection curve for S11 and S13.

by Miah and Kabir [7] to verify the results of the finite element model. Figures 5 and 6 illustrate the load–deflection curves for S1 and S2 slabs. Table 2 shows the cracking load, ultimate load, and maximum mid-span deflection of S1 and S2 slabs. The results of the finite element method clearly showed good agreement with the other

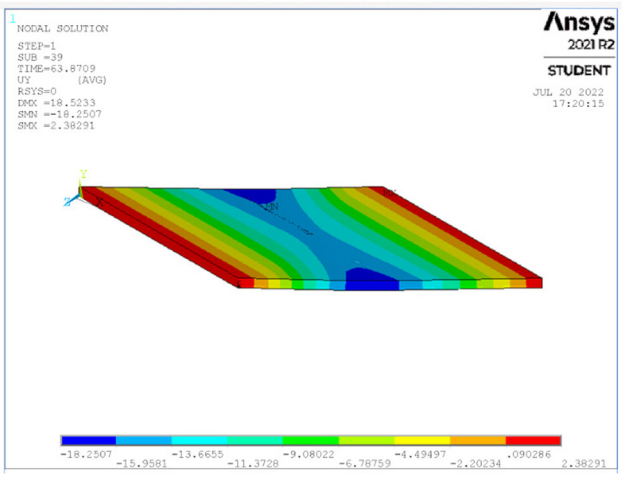

Figure 15: Deflection at ultimate load for S2.

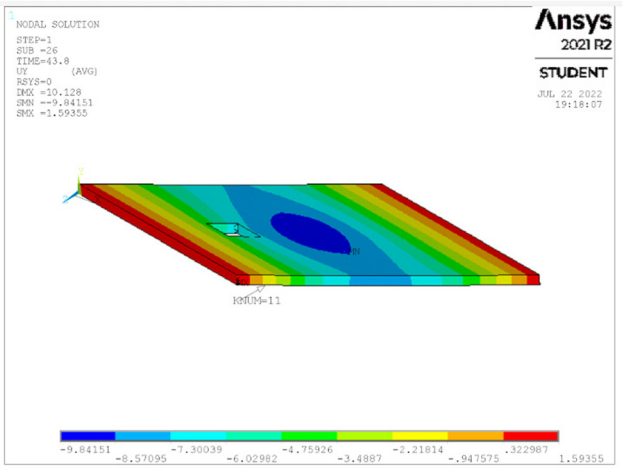

Figure 16: Deflection at ultimate load for S3.

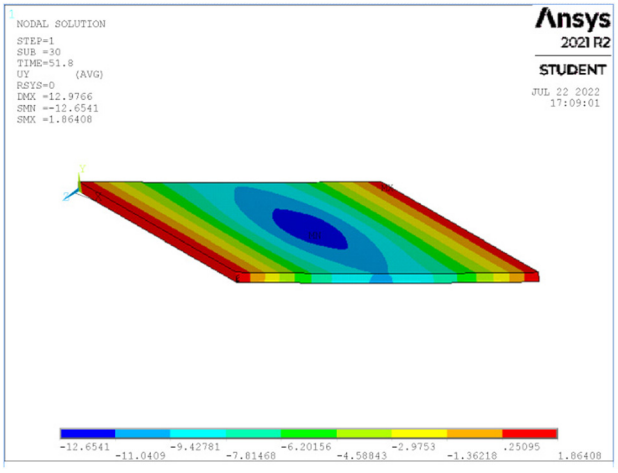

Figure 14: Deflection at ultimate load for S1.

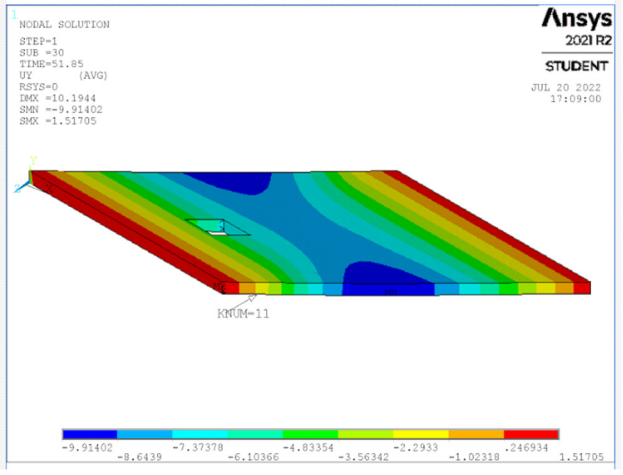

Figure 17: Deflection at ultimate load for S4.

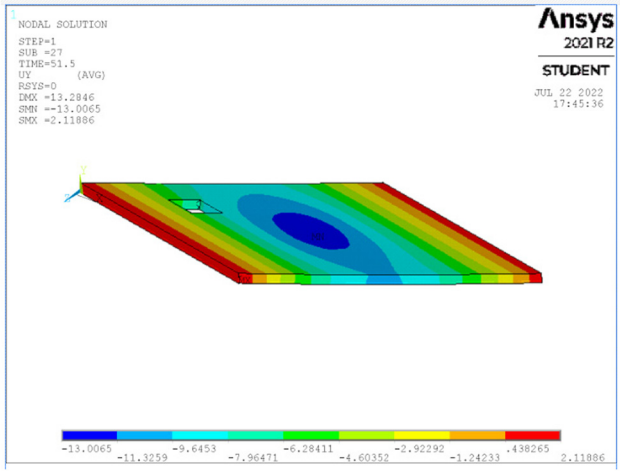

Figure 18: Deflection at ultimate load for S5.

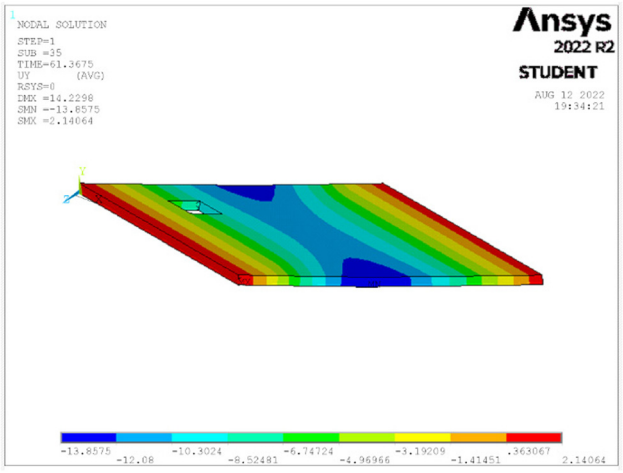

Figure 19: Deflection at ultimate load for S6.

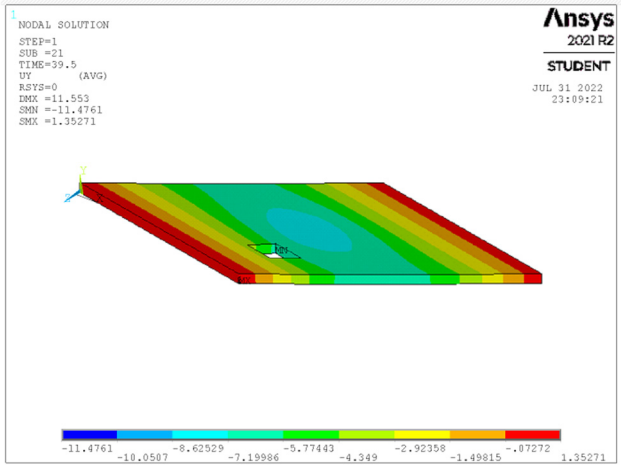

Figure 20: Deflection at ultimate load for S7.

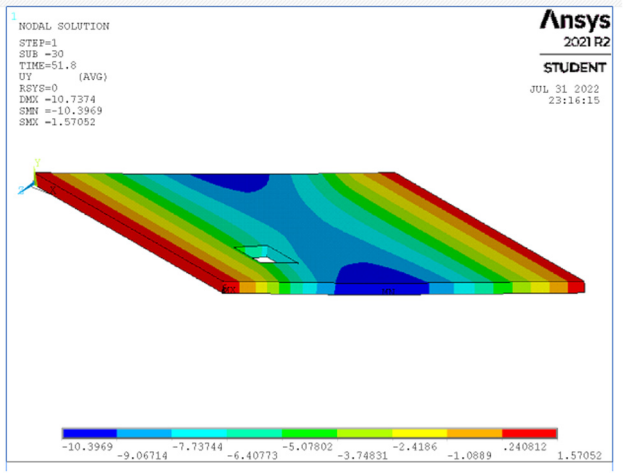

Figure 21: Deflection at ultimate load for S8.

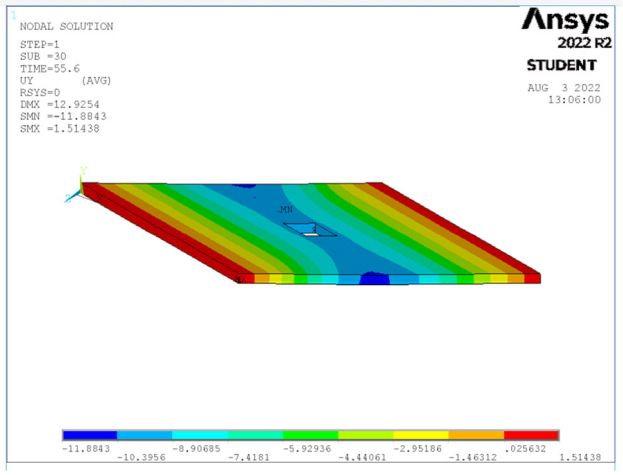

Figure 22: Deflection at ultimate load for S9.

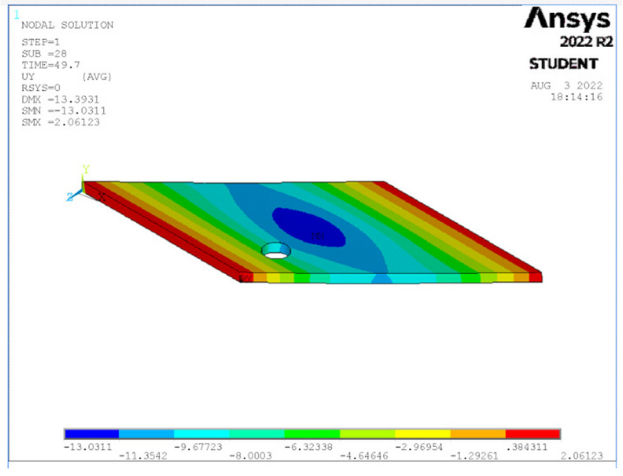

Figure 23: Deflection at ultimate load for S10.

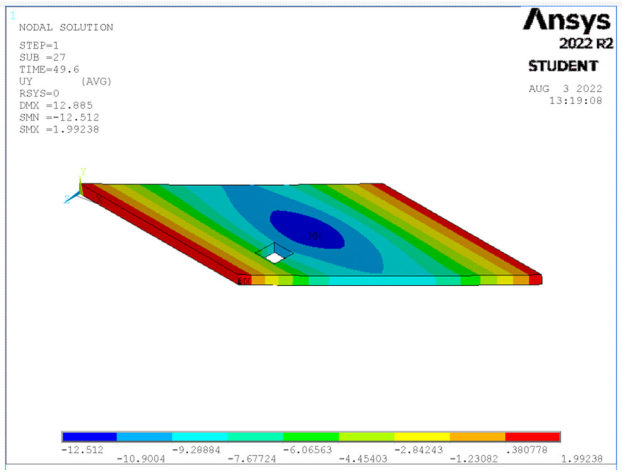

Figure 24: Deflection at ultimate load for S11.

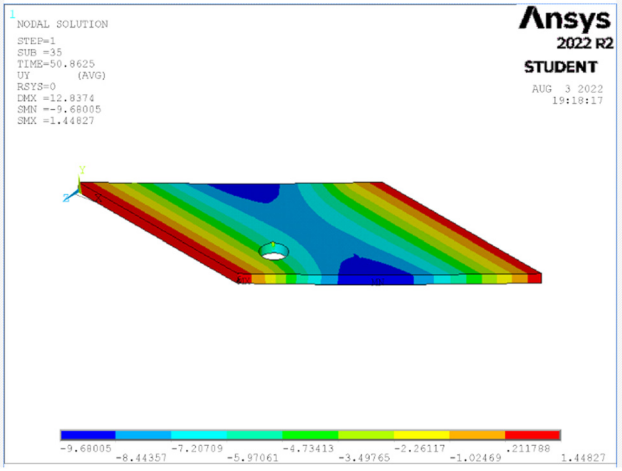

Figure 25: Deflection at ultimate load for S12.

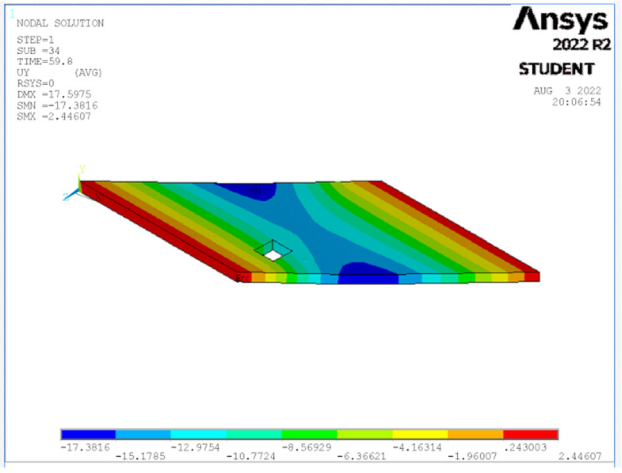

Figure 26: Deflection at ultimate load for S13.

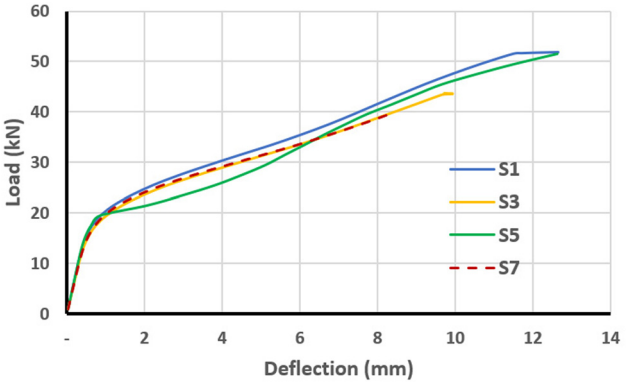

Figure 27: Load–deflection curves for slabs with one-point loading and openings located in different positions.

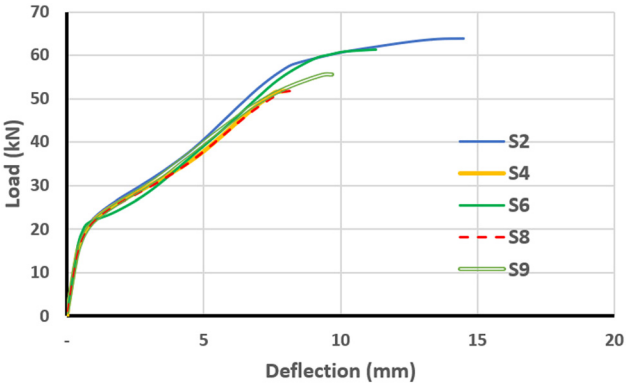

Figure 28: Load–deflection curves for slabs with four-point loading and openings located in different positions.

ults, which gives confidence in the finite element model. The strength is typically overstated by finite elements. This is because the boundary conditions of the finite element model are stiffer than those of the actual structure, and the materials in the model are homogeneous, in contrast to those in the experimental test. The microcracks that drying shrinkage can cause are not taken into account by the models. Additionally, in the calculations using finite elements, a perfect link between the steel reinforcement and the concrete is assumed. For the experimental specimen, there is some slippage, though [30].

5 Studied cases

Thirteen cases of skew slabs were considered in this study, including two loading types (one-point loads and four-point loads), different opening positions, and different shapes of opening with an equivalent area. Figure 7 and Table 3 illustrate the details of these cases.

Table 4: Results of slab cases for different opening positions under one-point loading

Skew slab ID	First crack load (kN)	% Difference of first crack	Ultimate load (kN)	% Difference of ultimate load	Midspan deflection (mm)	% Difference of mid span deflection
S1	9.5	0	51.8	0	12.7	0
S3	3.5	−63.2	43.8	−15.4	9.7	−23.6
S5	11.5	21.1	51.5	−0.6	12.6	−0.8
S7	2	−78.9	39.5	−23.7	8.3	−34.6

Table 5: Results of slab cases for different opening positions under four-point loading

Skew slab ID	First crack (kN)	% Difference of first crack	Ultimate load (kN)	% Difference of ultimate load	Midspan deflection (mm)	% Difference of midspan deflection
S2	11.5	0	63.9	0	14.5	0
S4	7.5	−34.8	51.85	−18.9	8	−44.8
S6	13.5	17.4	61.4	−3.9	11.3	−22.1
S8	3.5	−69.6	51.8	−18.9	8.2	−43.4
S9	9.5	−17.4	55.6	−13.0	9.7	−33.1

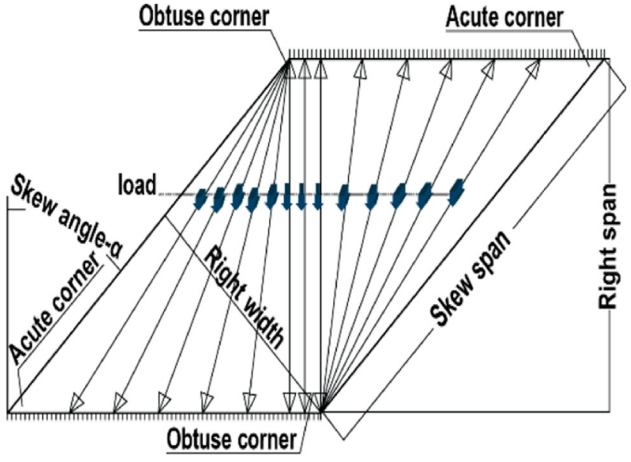

Figure 29: Effective load transfer pathway [31].

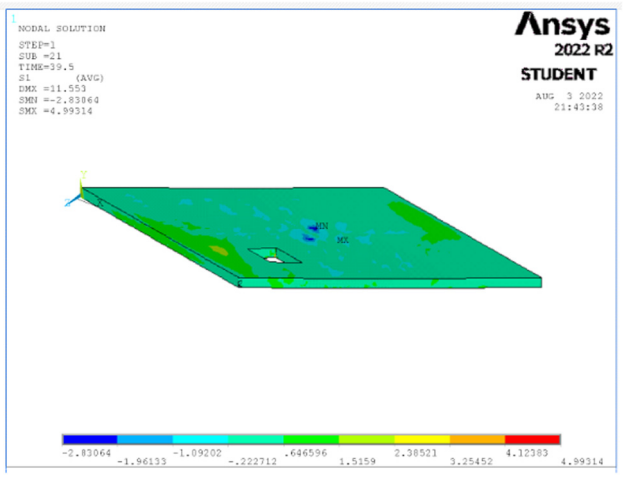

Figure 30: Stresses at ultimate load in first principal direction for S7.

6 Results and discussion

6.1 Effect of loading

It is evident from Figures 8–13 that the four-point loading achieves a higher ultimate load and deflection than the one-point loading. The reason is that the four-point loading distributes the load more effectively over the skew slab. The load–deflection curves depicted in these figures generally behave in a manner that is approximately identical to the linear stage. After that, they display greater stiffness for the four-point loading. The maximum difference of the ultimate mid-span deflection between one-point and four-point loaded slabs with the same opening

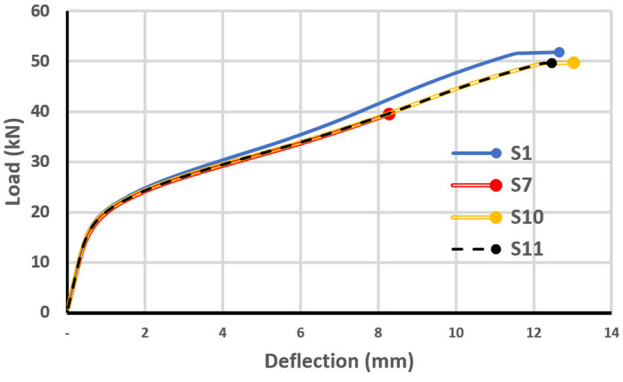

Figure 31: Load–deflection curves for slabs with one-point loading with different shapes of opening.

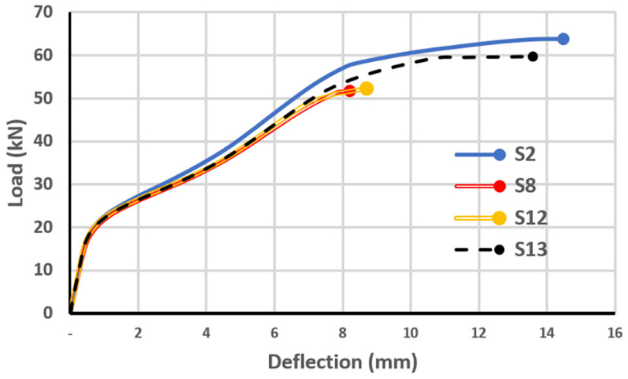

Figure 32: Load–deflection curves for slabs with four-point loading with different shapes of opening.

was recorded in the comparison of slabs S10 and S12 (Figure 12).

The deflection of all studied cases of the skew slabs is shown in Figures 14–26 for each case at the maximum load. When a single point is loaded, the maximum deflection is seen in the middle of the slab. When a four-point load is applied, however, the maximum deflection is visible at both edges of the slabs' middle span.

6.2 Effect of the position of the opening

The load–deflection curves for different positions of skew opening are shown in Figures 27 and 28. Table 4 illustrates that, for one-point loading, the opening has a negligible effect on ultimate load and deflection when it is located near the acute corner (S5), but has the maximum effect when located near the obtuse corner (S7), where it lowers the ultimate load by 23.7% and the deflection at ultimate load by 34.6% compared with a slab with no opening. When the opening is located at the position of (S3), the ultimate load and deflection decrease by 15.4 and 23.6%, respectively, compared with a slab with no opening. Meanwhile, slab S5 was able to withstand the largest load before the initial crack manifested (at 11.5 kN), whereas a crack developed in slab S7 with a loading of only 2 kN.

For four-point loading, the results in Table 5 show that there is only a slight effect on ultimate load and deflection when the opening is located near the acute corner (S6) the same as for one-point loading but has the maximum effect when the opening is located near the obtuse corner (S4 and S8). Specifically, when the opening is located near the obtuse corner (S8), ultimate load and deflection are reduced by 18.9 and 43.4%, respectively, compared with a slab with no opening. Meanwhile, when the opening is located at the position of S4, the ultimate load and deflection decrease by 18.9 and 44.8%, respectively, compared with a slab with no opening. The minimal effect on structural integrity associated with openings located near the acute corner (S6) could be because the applied load on the skew slab tries to transfer to the supports with the minimum energy. This means that the load path in such a structure tends to take the shortest path possible to the supports at the obtuse corners of the slab spans [31], as shown in Figure 29. It was also noticed that when the opening was located near

Table 6: Results of slab cases for different opening shapes under one-point loading

Slab ID	First crack load (kN)	% Difference of first crack	Ultimate load (kN)	% Difference of ultimate load	Midspan deflection (mm)	% Difference of midspan deflection
S1	9.5	0	51.8	0	12.7	0
S7	2	−78.9	39.5	−23.7	8.3	−34.6
S10	9.5	0.0	49.7	−4.1	13	2.4
S11	7.5	−21.1	49.6	−4.2	12.5	−1.6

Table 7: Results of slab cases for different opening shapes under four-point loading

Slab ID	First crack (kN)	% Difference of first crack	Ultimate load (kN)	% Difference of ultimate load	Midspan deflection (mm)	% Difference of midspan deflection
S2	11.5	0	63.9	0	14.5	0
S8	3.5	−69.6	51.8	−18.9	8.2	−43.4
S12	11.5	0.0	52.3	−18.2	8.7	−40.0
S13	9.5	−17.4	59.8	−6.4	13.6	−6.2

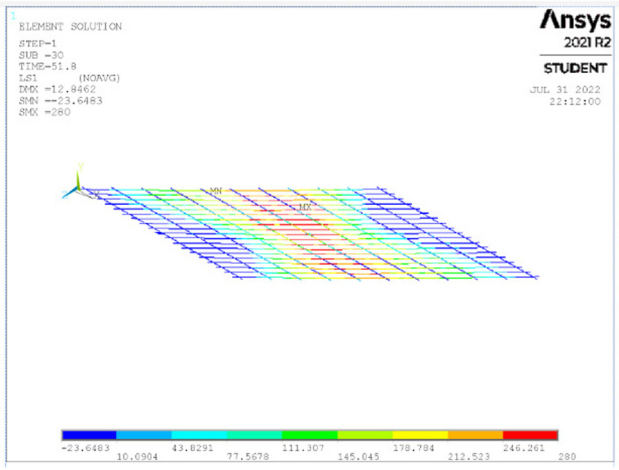

Figure 33: Steel reinforcement stresses at ultimate load for S1.

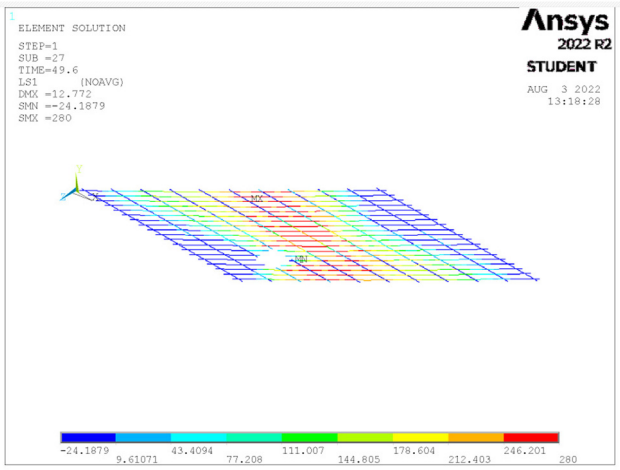

Figure 35: Steel reinforcement stresses at ultimate load for S11.

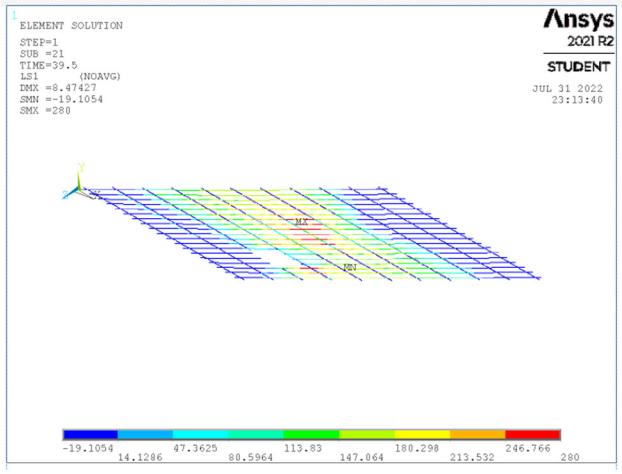

Figure 34: Steel reinforcement stresses at ultimate load for S7.

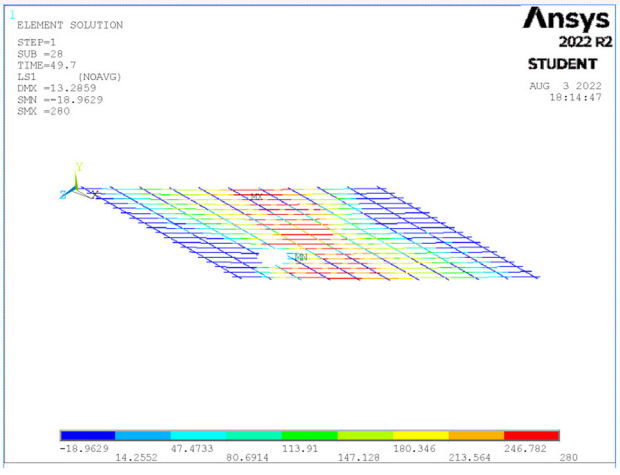

Figure 36: Steel reinforcement stresses at ultimate load for S10.

the obtuse corner negative cracking was induced near the opening toward the supports, as shown in Figure 30, causing a reduction in skew slab strength.

6.3 Effect of opening shape

Three shapes of openings with the same area were selected in this study: skew, circle, and rectangular shapes. The skew opening had dimensions of 200 mm × 200 mm, the circle had a radius of 950 mm, and the rectangular had dimensions of 170 mm × 170 mm. The location of these openings was chosen to be near the obtuse corner because this location has more effect on the skew slab strength, as discussed in the previous section. Here, it was evident that the effect of the opening depends mainly on the steel removed, and the negative cracks appear due to the opening. Figures 31 and 32 show the load–deflection curves for different shapes of opening for one-point and four-point loading, respectively.

The skew shape opening depicts more reduction in slab strength than other shapes (by 78.9 and 69.6% for one-point and four-point loading, respectively, compared with a slab with no opening, as shown in Tables 6 and 7). In one-point loading, circular and rectangular openings introduce approximately the same amount of strength reduction, which was about 4%. In contrast, in the four-point loading, the rectangular opening recorded better performance than other opening shapes, as shown in Table 7.

Figures 33–35 show the distribution of steel reinforcement stresses at ultimate load under the different types of openings (Figure 36).

7 Conclusion

The main conclusions that can be drawn from the current study are as follows:

1. When four-point loading is applied, the skew slab behaves more stiffly and has higher ultimate strength than under one-point loading due to the more efficient distribution of the load.
2. The skew slab is sensitive to the location of the opening. While all opening positions cause a decrease in the strength of the skew slab, the biggest reduction in strength occurs when the opening is located in the region between the obtuse corners of the skew slab, which is the region in which most of the load is transferred. Engineers should therefore take care to determine the suitable location for the opening.
3. Given the same opening location, the skew slab's strength is also affected by the shape of the opening, with the skew opening reducing the ultimate strength by more than the square and circle openings.
4. The impact of the opening shape also depends on how many steel reinforcements are removed and the appearance of negative cracking brought on as a result of the opening.
5. Negative steel reinforcement is highly recommended when an opening is needed in a skew slab to prevent cracking and maintain the slab's strength.

Conflict of interest: Authors state no conflict of interest.

References

[1] Moya L, Lantsoght EO. Parametric study on the applicability of AASHTO LRFD for simply supported reinforced concrete skewed slab bridges. Infrastructures. 2021 Jun 16;6(6):88.

[2] Ismail E. Distribution of stresses and displacements in skewed concrete slabs. MSc thesis. Linnaeus University, Faculty of Technology; 2017.

[3] Abozaid LA, Hassan A, Abouelezz AY, Abdel-Hafez LM. Nonlinear behaviour of a skew slab bridge under traffic loads. World Appl Sci J. 2014;30(11):1479–93.

[4] Huang H, Shenton HW, Chajes MJ. Load distribution for a highly skewed bridge: Testing and analysis. J Bridge Eng. 2004 Nov;9(6):558–62.

[5] Menassa C, Mabsout M, Tarhini K, Frederick G. Influence of skew angle on reinforced concrete slab bridges. J Bridge Eng. 2007 Mar;12(2):205–14.

[6] Sindhu BV, Ashwin KN, Dattatreya JK. SV D. Effect of skew angle on static behaviour of reinforced concrete slab bridge decks. Int J Res Eng Technol. 2013 Nov;2(1):50–8.

[7] Miah MK, Kabir A. A study on reinforced concrete skew slab behavior. J Civ Eng (IEB). 2005 Dec;33(2):91–103.

[8] Sharma M. Finite element modelling of reinforced concrete skew slab. ME (Structures) thesis. Punjab: Thapar University Patiala; 2011.

[9] Minalu KK. Finite element modelling of skew slab-girder bridges. M. Sc. D. thesis. Faculty of Civil Engineering and Geosciences, Delft University of Technology; 2010.

[10] Théoret P, Massicotte B, Conciatori D. Analysis and design of straight and skewed slab bridges. J Bridge Eng. 2012 Mar 1;17(2):289–301.

[11] Boobalan SC, Abirami P, Indhu K. Numerical examination of reinforced concrete skew slabs. Int J Innov Technol Explor Eng. 2020;9(5):512–6.

[12] Sharma M, Kwatra N, Singh H. Modelling of flexural response of simply supported RC skew slab. Curr Sci. 2020 Jun 25;118(12):1911.

[13] Singh A, Kumar A, Khan MA. Effect of skew angle on static behavior of reinforced concrete slab bridge decks: A review. In Res J Eng Technolo. 2016;3:1537–9.

[14] Roll F, Aneja I. Model tests of box-beam highway bridges with cantilevered deck slabs. ASCE Transportation Engineering Conference; 1966 Oct 17.

[15] Khaleel MA, Itani RY. Live-load moments for continuous skew bridges. J Struct Eng. 1990 Sep;116(9):2361–73.

[16] Khatri V, Maiti PR, Singh PK, Kar A. Analysis of skew bridges using computational methods. Int J Comput Eng. 2012 May;2(3):628–36.

[17] Kar A, Khatri V, Maiti PR, Singh PK. Study on effect of skew angle in skew bridges. Int J Eng Res Dev. 2012 Aug;2(12):13–8.

[18] Kothari V, Murnal P. Seismic analysis of skew bridges. J Civ Eng Environ Technol. 2015;2(10):71–6.

[19] Anusreebai SK, Krishnachandran VN. Effect of skew angle on the behaviour of skew slab under uniformly distributed load. Int J Res Appl Sci Eng Technol. 2016;3(8):1879–85.

[20] Hussein MJ, Jabir HA, Al-Gasham TS. Retrofitting of reinforced concrete flat slabs with cut-out edge opening. Case Stud Constr Mater. 2021 Jun 1;14:e00537.

[21] Oukaili NK, Merie HD. CFRP strengthening efficiency on enhancement punching shear resistance of RC bubbled slabs with openings. Case Stud Constr Mater. 2021 Dec 1;15:e00641.

[22] Al-Rousan R. Influence of opening sizes on the flexural behavior of heat-damaged reinforced concrete slabs strengthened with CFRP ropes. Case Stud Constr Mater. 2022 Dec 1;17:e01464.

[23] Kohnke P. Ansys mechanical apdl and mechanical applications theory reference. Canonsburg, Pennsylvania, U.S.A.: Ansys. Inc.; 2010.

[24] ANSYS. ANSYS Theory Reference. Southpointe: ANSYS, INC.: 2001.

[25] ANSYS release version 11 A Finite element computer software theory and user manual for nonlinear structural analysis. Canonburg, PA: Ansys Inc.; 2007.

[26] Desayi P, Krishnan S. Equation for the stress-strain curve of concrete. J Proc. 1964;61(3):345–50.

[27] Suhaib YKA-D. Effects of concrete nonlinear modeling on the analysis of push-out test by finite element method. J Appl Sci. 2007 May;7(5):743–7.

[28] Ibrahim KA. Investigating the effect of the repeated loads on the behavior of joint in A bridge between steel and concrete sections. Ph.D. thesis. Civil Engineering Department, University of Mosul; 2022.

[29] Bathe KJ. Finite element procedures. New Jersey: Prentice-Hall, Inc; 1982. p. 1052.

[30] Chansawat K. Nonlinear finite element analysis of reinforced concrete structures strengthened with FRP laminates. Oregon State University; 2003.

[31] Mohseni I, Cho YK, Kang J. Live load distribution factors for skew stringer bridges with high-performance-steel girders under truck loads. Appl Sci. 2018 Sep 21;8(10):1717.